Geomechanics and Engineering, *Vol. 28, No. 6 (2022) 613-624*
https://doi.org/10.12989/gae.2022.28.6.613

Study on the water bursting law and spatial distribution of fractures of mining overlying strata in weakly cemented strata in West China

Yangyang Li[1,2], Shichuan Zhang*[1,2], Yingming Yang[1], Hairui Chen[3], Zongkai Li[4] and Qiang Ma[4]

[1]*State Key Laboratory of Water Resource Protection and Utilization in Coal Mining, Beijing, 102209, China*
[2]*State Key Laboratory of Mining Disaster Prevention and Control, Shandong University of Science and Technology, Qingdao, Shandong Province, 266590, China*
[3]*Shaanxi Zhengtong Coal Industry Co., Ltd, Xianyang, Shaanxi Province, 713600, China*
[4]*Lin Yi. Shandong Energy Mining Group Co., Ltd, Linyi, Shandong Province, 276017, China*

(Received June 1, 2021, Revised August 14, 2021, Accepted September 27, 2021)

Abstract. A study of the evolution of overburden fractures under the solid-fluid coupling state was conducted based on the geological and mining characteristics of the coal seam depth, weak strata cementation, and high-intensity mining in the mining areas of West China. These mining characteristics are key to achieving water conservation during mining or establishing groundwater reservoirs in coal mines. Based on the engineering background of the Daliuta Coal Mine, a non-hydrophilic simulation material suitable for simulating the weakly cemented rock masses in this area was developed, and a physical simulation test was carried out using a water-sand gushing test system. The study explored the spatial distribution and dynamic evolution of the fractured zone in the mining overburden under the coupling of stress and seepage. The experimental results show that the mining overburden can be vertically divided into the overall migration zone, the fracture extension zone and the collapse zone; additionally, in the horizontal direction, the mining overburden can be divided into the primary fracture zone, periodic fracture zone, and stop-fracture zone. The scope of groundwater flow in the overburden gradually expands with the mining of coal seams. When a stable water inrush channel is formed, other areas no longer generate new channels, and the unstable water inrush channels gradually close. Finally, the primary fracture area becomes the main water inrush channel for coal mines. The numerical simulation results indicate that the overlying rock breaking above the middle of the mined-out area allows the formation of the water-conducting channel. The water body will flow into the fracture extension zone with the shortest path, resulting in the occurrence of water bursting accidents in the mining face. The experimental research results provide a theoretical basis for the implementation of water conservation mining or the establishment of groundwater reservoirs in western mining areas, and this theoretical basis has considerable application and promotion value.

Keywords: mining disturbance; solid-fluid coupling; spatial fracture of mining overlying strata; water bursting law; weakly cemented strata

1. Introduction

China is the world's largest coal-producing country and leads the world in coal production and consumption. Compared with coal resources in the eastern region of China, coal resources in the western region are abundant. In the western region, the geology and hydrology are relatively simple, coal seam conditions are relatively stable, and the coal seam depths are shallow. The bedrock is thin, and the surface is mostly covered by wind-borne sand in the western region. This simple geological condition can be exploited to implement high-intensity mining (Khorasani *et al.* 2019), such as fully mechanized longwall mining or mining with a large mining height. However, compared with mining in the eastern region, due to the shallowly buried and weakly cemented soft rock layer, the movement of the roof rock layer is particularly sensitive and strong in the horizontal and vertical directions. It is also difficult for the overlying rock to form a large structure during actual mining. The movement and deformation of the strata are relatively significant, and the caving zone and the water-conducting fracture zone are fully developed (Lu *et al.* 2018). Mining fractures can even directly penetrate the ground surface (Kratzsch 1983), forming large-scale ground fractures, step subsidence and other noncontinuous deformation failures (Whittaker 1989), and this leads to soil and water loss, water level decline (Peng 1992), surface vegetation degradation, and land desertification (Liao *et al.* 2013).

The coal seams in mining areas of Central and East China are generally Carboniferous Permian coal seams, and the overlying strata of these coal seams are thick loose stratum. For the mining in this area, experiments and research were carried out on the development height of the caving zone and the water conducted fracture zone, and many results were obtained. These data provide theoretical support for guiding the determination of the mining upper limit and the determination of the water conducted fracture zone (Bai and Elsworth 1990, Ning *et al.* 2017). For example, Hu *et al.* (2016) obtained a few phases of measured data based on surface movement observation

*Corresponding author, Ph.D.
E-mail: 373260186@qq.com

ISSN: 2005-307X (Print), 2092-6219 (Online)

stations and analyzed the mechanism of surface movement and deformation with the combination of key stratum theory (Lu *et al.* 2020), mining and geological conditions, which provide a theoretical reference for land reclamation and ecological restoration under the condition of high-intensive mining in the windy and sandy region. Zhang *et al.* (2020) identified the development of the fracture zones caused by water flows and ensured the mining safety and protection of groundwater in shallow coal seams beneath gully topography by using comparative approaches, including physical simulations, numerical simulations. However, the research results are only applied to the eastern mining areas in China, but not to the western mining areas.

The above scholars often carried out related research on eastern mining areas, although the existing traditional "three-zone" theory (Cheng *et al.* 2017) and mine pressure theory (Komurlu *et al.* 2015) are not completely suitable for the specific mining geological conditions in the western mining areas. The coal seams mined in the eastern areas are thin, and medium-thick coal seams are formed under the condition of hard and medium hard overburden rock. In the study of the evolution and mechanism of mining fractures, the analysis and prediction methods are still unclear. The existing empirical formulas for water-conducted fracture zones are not suitable for high-intensity mining in the west. For example, Zhang *et al.* (2013) researched the influence of face advancing length on the height of the water-flowing fracture zones, and a deep coal mine with a large dip was chosen as the research object to establish an in-house experimental system of similar simulation to obtain the mining-crack-evolution characteristics of the overburden strata; however, most of the above results were obtained by numerical simulation and general physical simulation and did not consider the solid fluid coupling environment. Thus, these results are not applicable to western coal mines and the overburden breaking and fracture evolution rules and spatial distribution in western mining areas must be further investigated.

Comprehensive mechanized longwall mining is adopted in western mining areas. Compared with eastern mining areas, the mining intensity in western mining areas is higher and the coal seams are buried at shallower depths, which leads to overburden movement and intense deformation. The cracks in overburden rock can even directly penetrate the surface, forming large-scale ground fissures, bench subsidence and other surface discontinuous damage, which result in soil erosion, water level drops, surface vegetation degradation and land desertification. Therefore, it is very important to study the evolution characteristics of fractures in overburden areas. The physical simulation and observation of the mining crack evolution process is an important approach in researching the overburden strata movement in a solid fluid coupling environment (Li *et al.* 2017) and can compensate for the deficiencies of numerical simulation methods (Annaidh *et al.* 2013). In the solid-liquid coupling simulation test, the most important step is the selection of nonhydrophilic similar simulation materials. Zhang *et al.* (2017) developed appropriate fluid–solid coupling materials and proposed materials for simulating the coal mine floor rock. These research results facilitate physical simulation experimental studies of solid fluid coupling in the laboratory.

For mining-induced fracture development with groundwater interaction, scholars in other coal regions have also carried out a considerable amount of research. Schubert (1980) suggested that the larger inflows possibly could be avoided if the structural control of fractures in coal basins is better understood. Such work provides a direction for the research in this field. Ouyang and Elsworth (1993) used a modulus reduction ratio to represent strata deformation and concurrent steady fluid flow in a naturally fractured medium as a result of underground mining, and they revealed that changes in strata conductivities are strongly related to deformations induced by underground mining; therefore, the study of overlying rock fracture distribution has become the focus of roof water inflow. Bruce (2020) discussed the parameter often referred to as “height of fracturing” in terms of the critical parameters that influence it, and the relevance of groundwater impacts in the southern coalfields of New South Wales, south of Sydney. Morrison *et al.* (2019) investigated a small waterway that had been impacted by upwelling groundwater due to recent geological strata fracturing caused by longwall coal mining on the southwestern outskirts of Sydney. The above research results do not discuss the influence of the overlying strata movement process during mining, and few studies have focused on the formation of overlying rock fractures and their damage to the environment.

Based on the above problems and the actual needs of the project, a non-hydrophilic similar simulation material is developed aiming at the geological and mining characteristics of West China, and a water-sand gushing simulation test system is used. In this study, the 52505 working face of the Daliuta Coal Mine is used as the engineering background to study the spatial distribution and dynamic evolution of the fractured zone in the mining overburden under the coupling of stress and seepage. To analyze the rules of water flow in the loose stratum of the coal seam in the coal mining direction, the basis for the division of space-time zoning is proposed in addition to the regionalization of the movement of overlying strata in shallowly buried and weakly cemented strata. The experimental research results provide a theoretical basis for the implementation of water conservation mining or the establishment of groundwater reservoirs (Wang *et al.* 2019), such as the selection of reservoir locations and the determination of crack grouting methods, which have great application and promotion value.

2. Engineering background

The 52505 working face of the Daliuta Coal Mine is located in the No. 5 panel of the mine. The working face is located on the east side of the alley and west of the mine field border; the south side is the 52504 working face, and the north side is the undeveloped solid coal body. The coal mining method is a comprehensive mechanized mining method with a designed overall height of mining that is achieved at a certain time with the caving backward mining

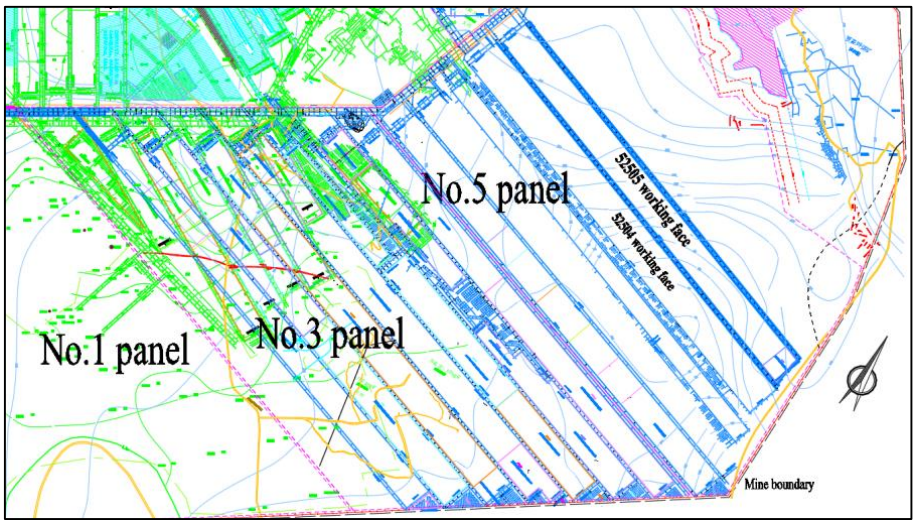

Fig. 1 Location of the 52505 working face in the Daliuta Coal Mine

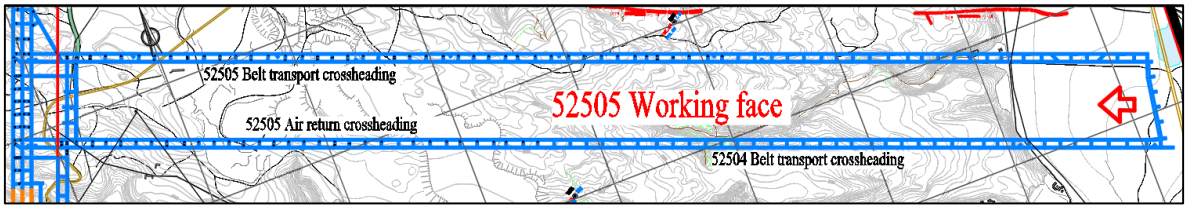

Fig. 2 Roadway layout of the 52505 working face

Table 1 Comprehensive histogram of the rock strata in the 52505 working face

Horizon	Rock name	Max and Min/m	Layer thickness/m	Cumulative thickness/m	description
1	Loose layer	0~50	30	30	Loose layers are mainly composed of aeolian sand, fixed sand, sandy clay, gravelly sand, etc.
2	Siltstone, fine sandstone	10~30	20	50	Mainly powder and fine sandstone, with mudstone or medium and coarse sandstone.
3	Silty sandstone e	20.1~142.5	120	170	An argillaceous cemented clastic rock system consisting mainly of fine sandstone.
4	Fine sandstone	2.9~21.8	12.7	182.7	Off-white, sorting, etc., roundness is good, and the main component is quartz.
5	Siltstone	0~2.8	1.3	184	Gray, microwave-like bedding, muddy cementation, rich in plant fossils.
6	5-2 coal	7.10 ~ 7.30	7.25	191.35	Coal and rock types are mainly semi-dark and semi-bright, and some are dim and bright briquettes.
7	Siltstone	1.7 ~ 5.2	2.8	194.15	Gray, muddy cementation, horizontal bedding development, thin layers of mudstone and coarse sandstone development.

type. The 52505 working face adopts the natural caving method to handle the goaf.

The specific location of the 52505 working face is shown in Fig. 1. The surface ground elevation is 1083.4~1229.3 m, the floor elevation is 981.32~1032.76 m, the length of the working face is 4268.80 m, the width is 301.3 m, and the area is 1.282 million m^2. There is no fault structure in the working face. The 52505 working face is mined in the 5-2 coal seam, the coal thickness is 7.1~7.3 m, the average is 7.25 m, and the coal seam inclination angle is 1~3°. The comprehensive histogram of rock strata in the 52505 working face is shown in Table 1. The working face is located in the five panels of the 5-2 coal seam. The 52505 return air crossheading is mainly used for return air and material transportation, and the 52505 belt transport crossheading is used for transporting coal and pedestrians. The design and layout of the roadway in the 52505 working face is shown in Fig. 2.

3. Simulation test scheme design

Due to the complexity of mining geological conditions, many factors affect mining engineering mechanics. Some

Fig. 3 Physical map of the test system

field problems cannot obtain satisfactory results by computer numerical simulations alone and cannot completely and accurately reflect the strata movement caused by mining. Therefore, physical similarity simulation experiments still play an important role in the process of mining engineering research by virtue of their advantages in simulating overburden movement.

3.1 Test equipment selection

In this paper, a simulation test system for mining overburden water gushing and sand breaking disasters (a water-sand gushing simulation test system) independently designed and developed by Shandong University of Science and Technology is used for testing. The test system is mainly composed of a main body frame, a transparent plate, a pressurized confined sump, an energy storage tank, a simulated mining device, a hydraulic pressure and water volume dual-servo system, a displacement stress dual-servo system and electrical control system; its main structure is shown in Fig. 3. Among these technologies, the system effectively simulates the size: length, width and height are 1200 mm, 400 mm and 700 mm, respectively.

A pressurized confined sump is set above the test bench and connected to the energy storage tank through a high-pressure hose, and a constant flow of water is injected by adjusting the hydraulic pressure water volume dual-servo system so that the test model is filled with permeated water. Considering the special requirement for the tightness of the test chamber and the impact of factors that are not mining-related on the test, the excavation of the coal seam on the site is simulated with a drawable steel plate (a simulated mining device). To visually observe the process of the experiment, transparent tempered glass plates are installed in front of the test bench to allow observation of the spatial structure of the overlying rock layer and the distribution of water channels after mining.

This system has the following characteristics:

(1) The simulation of the growth and development of the water bursting disaster has been realized;

(2) The water bursting channel can be formed under the action of mining and water pressure during the mining process, and the spatial structure, shape and size of the overburden are all formed spontaneously.

(3) The direct observation of deformation and failure of the overlying rocks, crack development and expansion, and formation of water channels during the mining of the working face is realized.

3.2 Determination of the test simulation parameters

The 52505 working face of the Daliuta Coal Mine is arranged along the tendency of the coal seam, with a width of 301.3 m, a mining length of 4268.80 m, and a designed mining height of 6.7 m. The choice of geometric similarity ratio is affected by many factors, such as the size of the test device, simulates the size effect of material strength. Referring to the geological mining conditions in the 52505 area and the effectiveness of the simulation experiment system (effective size: 1200 mm×400 mm×700 mm), the length of the similarity coefficient (C_L) of the model to prototype is designed to be 1:300. The similarity coefficient 1:300 is the optimal parameter in this study. The specific model characteristics are as follows:

(1) The physical simulation mining height is 22 mm, which is equivalent to the actual mining height of the project of 6.6 m, and the actual test needs to be simulated at 6.7 m;

(2) The physical model length is 1200 mm, which is equivalent to the actual projected length of 360 m;

(3) The physical model width is 400 mm, which is equivalent to the actual projected length of 120 m;

(4) The height of the physical model is 700 mm, which is equivalent to the actual overlying rock height of the project of 210 m.

3.3 Selection of test materials

The selection and proportion of similar materials have a great influence on the physical and mechanical properties of the model materials and play a decisive role in the success of the physical test. Most of the traditional materials used for similar models are sand, calcium carbonate, gypsum, etc. Models made of such materials undergo a large change in strength after being immersed in water and are easily disintegrated. Considering the particularity of simulation tests for water bursting disasters, low-strength and nonhydrophilic materials should be used to simulate rock masses to meet the needs of similar simulation tests.

The weakly cemented strata are mainly distributed in Ordos basin and Eastern Mongolia mining area in China (Sun *et al*. 2019). The degree of rock formation was not sufficient, thus the rock strength was generally low. In Western mining area, the lithology mainly included sandstone, sandy mudstone and mudstone. The strong disintegration of weakly consolidated rock is the main factor that causes the height of water conducting fracture zone to increase. The strength of weakly cemented rocks in Western mining area was lower than that of the same type rock in Middle Eastern mining area. Therefore, the developed similar simulation materials need to meet the characteristics of weakly cemented strata deformation.

With reference to the author's previous research results (Zhang *et al.* 2017), clean river sand, paraffin, calcium carbonate, Vaseline jelly and hydraulic oil were selected as

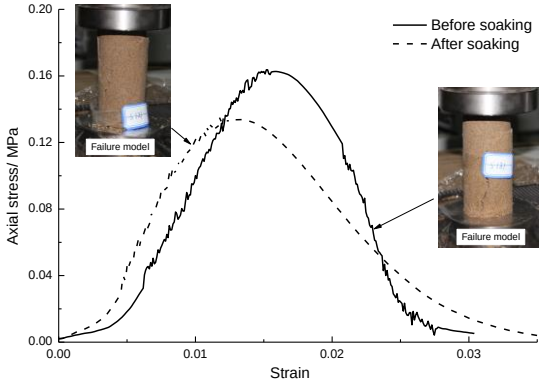

Fig. 4 Stress-strain curves and failure forms of typical simulated materials

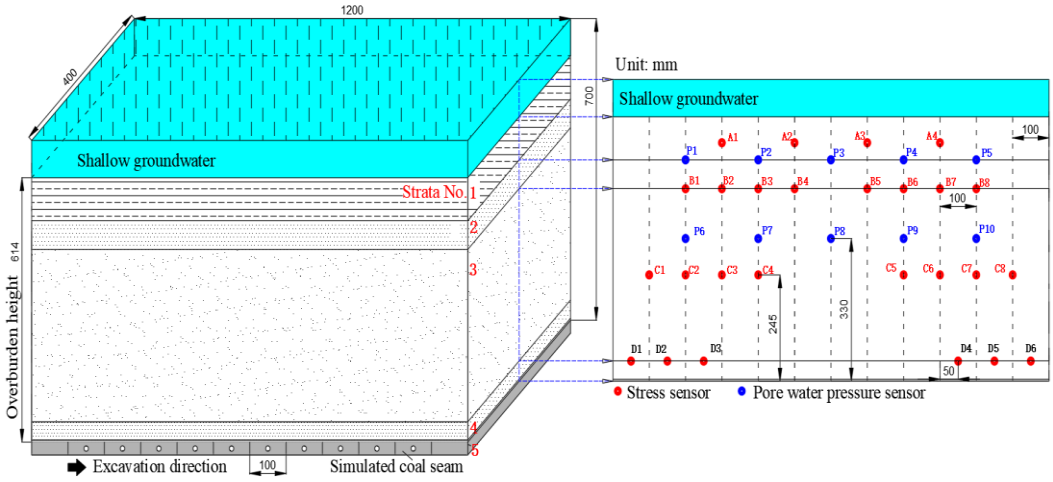

Fig. 5 3D mining model and sensor layout

the constituents of similar materials. The particle size of clean river sand is less than 0.3 mm, the dry sand density is 1.40 g/m^3, and the porosity is 0.41; paraffin wax is 58 % industrial crude paraffin, the melting point is 58~60℃, the density is 0.880-0.915 g/cm^3; Vaseline jelly is white and of nontoxic medical grade, its melting point is approximately 37~54℃ degrees, and the density is 0.815~0.830 g/cm^3. The blending agent is No. 46 anti-wear hydraulic oil with a density of 0.876 g/cm^3. Calcium carbonate is light calcium carbonate.

According to the test similarity ratio, the mass ratio ranges determined between the components of similar simulated materials were sand: paraffin wax = 40:0.5~1.5 and calcium carbonate: Vaseline jelly: hydraulic oil = 1:0.8~1.2:0.8~1.3. The uniaxial compression failure mode and stress-strain curve of the standard specimen before and after soaking are shown in Fig. 4. According to the indoor test, the compressive strength and permeability coefficients were controlled between 0.04 and 0.60 MPa and from 2.87×10^{-7} to 9.37×10^{-5} cm/s, respectiveely. The mechanical properties of the materials were similar to those of roof rocks, which were sufficiently nonhydrophilic. Their softening coefficient was in accordance with that reported in previous studies (Zhang *et al.* 2017). The mechanical properties of the similar material are similar to that of the actual roof rock, and they fit in with the required low strength and non-hydrophilicity for the test.

3.4 Test model layout and monitoring scheme design

(1) Similarity criteria and scale effect analysis

According to the comparison results of the test model and the mining prototype, the geometric similarity coefficient of the physical model is designed to be 1/300. The density of similar materials developed show that the weight similarity coefficient C_r of the model to prototype is 1/1.5. Based on the π theorem of similarity (Chen *et al.* 2019), the main similarity parameters were derived, and the stress similarity coefficient is calculated as $C_\sigma=C_rC_l=1/1.5\times1/300=1/450$. The model's permeability similarity coefficient is 11.5.

In the model test of similar materials, the laboratory test results of rocks were selected as the prototype parameters in the similarity theory. That is, the physical parameters of similar simulation materials refer to the indoor test results of overburden in 52505 working face, which is determined directly in the model. This process avoids the difference in the physical and mechanical parameters between rock in the laboratory and field and further reduces the influence of the scale effect on the test results.

Table 2 Basic mechanical information of the overburden and selection of the simulation material ratio

Layer number	Layer thickness/m	Simulated thickness/cm	Rock name	Density /kg/m^3	Compressive strength/MPa	Modulus of elasticity/GPa	Tensile strength/MPa	Poisson's ratio	Mass ratio
1	30.0	10.00	Loose layer	1960	3.88	0.40	0.40	0.27	40:0.5:1:1
2	20.0	6.67	Siltstone	2313	25.56	1.88	2.77	0.19	40:0.8:1:1
3	120.0	40.00	Silty sandstone	2204	37.64	3.88	2.43	0.23	40:1.2:1:1
4	12.7	4.23	Fine sandstone	2313	25.56	1.88	2.77	0.19	40:0.8:1:1
5	1.3	0.43	Siltstone	2370	14.25	2.20	1.75	0.26	40:0.8:1:1

(2) Three-dimensional mining model

Based on the actual geological mining environment of the coal mine, a three-dimensional mining model is designed, as shown in Fig. 5. Among different parameters, the simulated overburden height of the 3D model is 613.6 mm, and the thickness of the overburden at the site is 184.2 m. Four layers including one loose aquifer sand layer are laid on the roof of the coal seam from the bottom of the coal seam to the top of the coal seam. The physical simulated mining height is 22 mm, which is equivalent to the actual mining height of 6.7 m. The parameters of the simulated roof strata are shown in Table 2.

The mass ratios in Table 2 are the components of simulation materials (clean river sand, paraffin, calcium carbonate, Vaseline jelly and hydraulic oil in turn). During the test, to eliminate the boundary effect of the test model, a 100 mm × 400 mm steel plate is installed on each side of the coal seam, and it is not operated during the test, which is equivalent to leaving coal pillars of approximately 30 m on each side. Ten steel plates are installed in the coal seam excavation area. Each steel plate in the model is pulled out at a constant speed for 5 minutes, and mining is performed every 60 minutes, which is equivalent to the mining face advancing approximately 30 m per day. The total mining length of the whole model is 300 m. In this experiment, a smooth steel plate was placed between the test stand and similar materials to reduce frictional resistance and decrease boundary conditions errors.

(3) Sensor arrangement

A total of 26 BX-1 pressure sensors with a maximum observed value of 800 kPa were installed in the test model to monitor the dynamic change in the surrounding rock pressure during the mining process. 10 pore water pressure sensors (P1-P10), BS-1 sensors with an observed value of 2.5 MPa, were used to monitor the water flow in the overburden fractures. The experimental data were collected by a DH-3816N static strain measurement system at a sampling rate of 60 points per second, with a strain sensitivity coefficient of approximately 1.0 to 3.0. The layout locations of the sensors are shown in Fig. 5.

Among them, pressure sensors A1-A4 are located in the loose layer and are used to monitor the pressure change in the overlying rock near the surface; pressure sensors B1-B8 and C1-C8 are used to monitor the change in rock mass stress during crack formation in the main roof; pressure sensors D1-D6 are located at the bottom of the siltstone and are used to monitor the dynamic distribution characteristics of the surrounding rock abutment pressure during the mining process.

Fig. 6 3D mining model after layering

(4) Model layering process:

a. Before layering the test model, the simulated coal mining device was reset.

b. The weighed simulated materials were heated to 80°C and mixed well and then quickly poured into the test chamber for layering.

c. Between adjacent rock layers, rice paper was used as a natural layering boundary.

d. The sensors were placed into the test model and installed through the installation slot.

e. After the model layers were constructed, an external load was applied to improve compaction, and the model was left to dry for 2-5 days. The 3D mining model after layering is shown in Fig. 6.

f. With the model completely dry and the design finalized, the model was ready for corresponding loads to be exerted and hydraulic pressure to be applied.

4. Analysis and discussion of test results

4.1. Mining overburden collapse space and fracture evolution law

(1) Spatial distribution of collapse in the mining overburden

This test has a total of 10 steps (Steps 1-10), and the distance between each step of the excavation represents the actual coal mine 30 m. Fig. 7 shows the spatial distribution of overlying rocks at different excavation distances. The movement and deformation of the rock mass caused by mining are relatively significant, and the overburden damage has formed a large-scale surface deformation and movement.

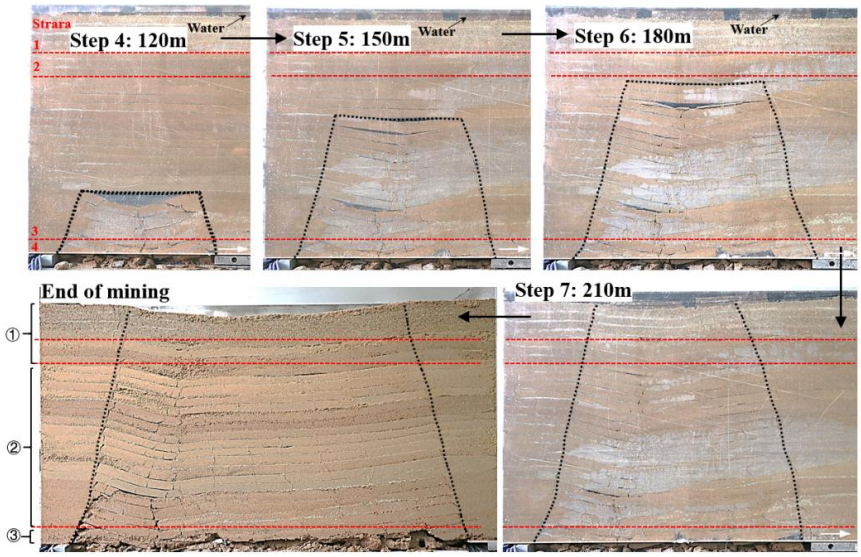

Fig. 7 Evolution law of the overburden collapse space under different excavation distances

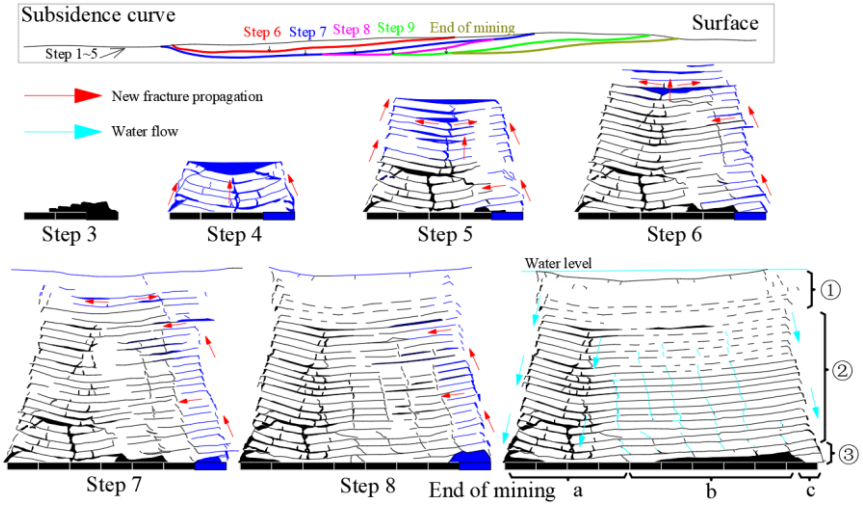

Fig. 8 Fracture evolutions of the overlying rock at different excavation distances. Blue indicates the newly formed fracture network after this step of excavation

During the excavation of Steps 1 and 2, the immediate roof (Strata 5, 1.3 m thick) collapsed with mining, and there was no obvious movement in the overlying strata. When the excavation reached Step 3, the 12.7 m basic roof (Strata 4) collapsed, and a small range of separation was formed between the strata at a short distance but did not cause a large movement zone (zone ③). Notably, due to the boundary effect of the test equipment, the vertical movement resistance of the model boundary material is relatively large, causing the basic roof to collapse when the excavation step reaches 60 m. These data are slightly larger than the actual collapse step of the actual project.

During the excavation of Step 4, the 120 m main roof (Strata 3) collapsed for the first time. The collapsed space showed a "trapezoidal distribution". The middle of the rock beam broke, and obvious connected cracks formed from the bottom of the coal seam to the top of the coal seam. The angle between the crack above the working face and the horizontal angle is 70°. When the excavation reaches Step 5, the collapse space expands in the horizontal and vertical directions. With each mining step, the roof breaking extends forward in the form of a “transferring beam”. When Step 6 is excavated, the falling space contacts the 20.0 m thick siltstone, and the overburden collapse space expands according to a certain rule (zone ②). When excavated to Step 7, the siltstone (Strata 2) and loose layer (Strata 1) are bent overall and moved as a whole (zone ①). At the same time, the collapse of the overlying rock affected the surface, causing the surface to sink and causing a significant drop in the water level.

According to the overlying rock collapse space after the excavation, it can be seen that the overlying rock collapse space affects the ground surface and is the direct cause of the drop in the surface water level. Due to the shallowly buried and weakly cemented soft rock layer in the upper part of the coal seam in West China, the movement of the roof rock layer is particularly sensitive and strong in the

horizontal and vertical directions. It is also difficult for the overburden to form a large structure during the actual mining process, and it is not possible to form an obvious "upper three zones" structure. Therefore, the collapse and movement of the mining overburden in shallow weakly cemented strata vary spatiotemporally and occur in certain zones in the vertical direction. According to the results of this test, the overburden can be divided into ① an overall migration zone, ② a fracture extension zone, and ③ a collapse zone, as shown in Fig. 7. The division method still needs many experiments and field observations.

(2) Fracture evolution in the mining overburden

Compared with the mining in the eastern region, the excavation intensity in the western region is greater, which is mainly reflected in the large mining height (> 6 m). At the same time, due to the influence of the shallowly buried and weakly cemented soft rock layer, the rock mass deformation is more significant. Water (sand) fracture zones are fully developed, and mining fractures can directly run though the ground surface, forming large-scale ground fractures and other surface damage, resulting in soil erosion and water level decline. To facilitate the analysis of the fracture development law in the overburden, the fracture distribution of the overburden under the excavation distance is sketched, as shown in Fig. 8.

When the excavation reaches Step 4, a fracture occurs in the middle of the rock beam, resulting in a large number of interconnected wide fractures in the overburden above the open-off cut, the working face, and the goaf, and this provides conditions for the formation of the water channel. When excavating Steps 5-7, new interlayer cracks and vertical penetrating cracks were successively formed above the fracture area formed by the initial collapse (i.e., Stage a). The width of the vertical penetrating crack was large, and did not easily close. As the working face continues to advance from Steps 7-9, the vertical fracture zone formed in the previous excavation above the working face is gradually closed by the periodic movement of the overburden. A new vertical fracture group is formed above the working face, so it enters Stage b. After Step 10, the vertical fracture group formed at the end of mining no longer closes and becomes a stable fracture group with a large degree of vertical conduction.

According to the results of this test, the overburden fractures in shallowly buried and weakly cemented strata have spatiotemporal zoning in the horizontal direction and can be divided into three zones: the primary fracture zone (a), the periodic fracture zone (b), and the stop-fracture zone (c) as shown in Fig. 8. Among them, there is a large range of interlayer fracture groups and vertical penetrating crack groups in zone (a). Zone a is always the main danger zone for water burst during the entire mining process; zones (b) and (c) are formed with advances in the working face, the fractures in zone (b) are closed to a certain extent due to periodic movement of overburden, and the danger is lower than that in zone (c); the vertical fracture group no longer closes in zone (c), which is the secondary water bursting danger area.

4.2 Variation characteristics of overburden stress

The change in the monitoring stress data during the experiment is shown in Fig. 9, where the abscissa is the test

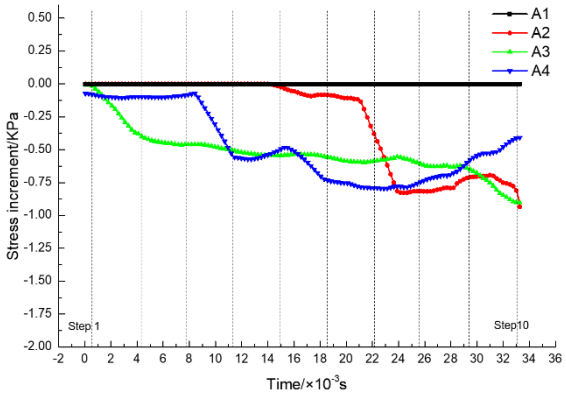

(a) Sensor stress change in the loose layer

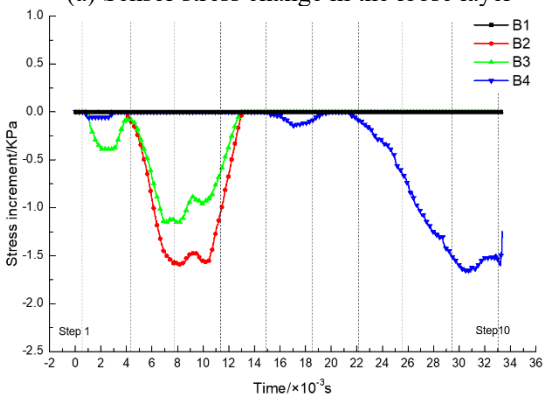

(b) Sensor stress change in the roof of Strata 3

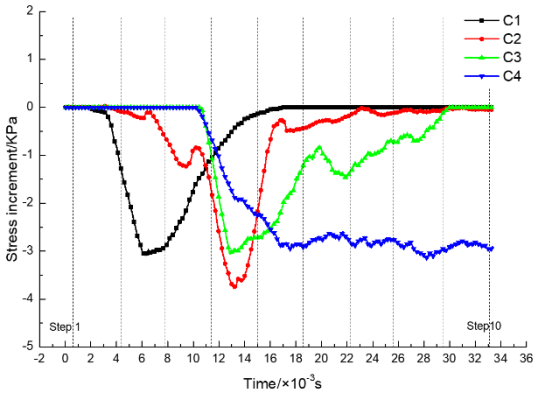

(c) Sensor stress change inside Strata

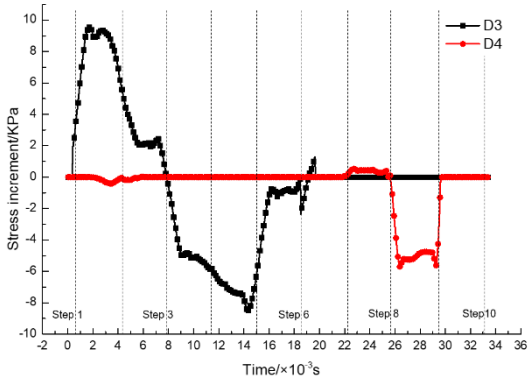

(d) Sensor stress change in the immediate roof

Fig. 9 Monitoring curves of the stress sensors at the different overburden locations

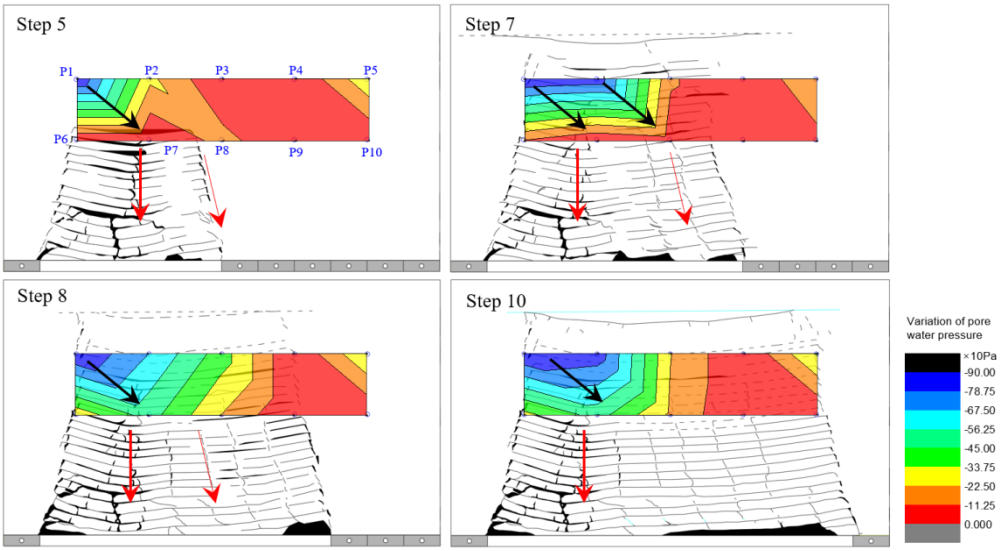

Fig. 10 Cloud diagrams of the pore water pressure changes in the different mining stages. The direction of the arrow indicates the direction of water flow, and the size of the arrow indicates the amount of water flow

time, and the dotted line corresponds to the time of 10 steps. Compared with other areas of overburden sensors, the stress change in the loose layer is smaller (Fig. 9(a)). There are two main reasons for this phenomenon: one is that the sensor is shallowly buried, and the other is that the siltstone (Strata 2) and loose layer (Strata 1) are bent and moved as a whole, resulting in less fracture space at the sensor location.

The monitoring data of Strata 3 are shown in Fig. 9(b) and Fig. 9(c). Because the B/C1-B/C4 and B/C5-B/C8 sensors are symmetrically distributed, the data have little similarity, so B1-B 4 and C1-C4 are selected for comparative analysis. As seen from the previous section, B1 is located outside the mining influence area, so no significant data changes have occurred. Under the coupling effect environment, a large separation occurs at the position of B2, causing the maximum change in the stress. With the excavation of the coal seam, the spatial extent of the separation layer increases, which in turn causes a sudden drop in B4.

The regularity of the stress change of the sensor in Strata 3 is more obvious, mainly in the following three aspects. First, the sensors at a close distance on the working face first undergo stress unloading, C1> C2> C3> C4, and as the working face advances, the sensors sequentially exhibit stress unloading. Second, the overlying rock integrity is high, and the rock mass in the main roof undergoes the process of unloading and then recovery. Third, the generation of overburden fractures greatly affects the change in stress in the rock mass, resulting in significant changes in the rock masses of this area, such as C3 and C4.

The stress changes monitored by the D3 and D4 sensors in the immediate roof are shown in Fig. 9(d). As the working face advances, the distance between the buried positions of D3 and D4 and the working surface is continuously shortened. The degree of mining influence is gradually increasing, the sensor indication is also increasing, and the change in D3 is higher than that in D4. At the moment the working face is past the buried position of the sensor, the sensor loses the support of the coal body, and the sensor indication also decreases rapidly. As the coal mining face continues to advance, the rock layer at the buried position of the sensor is gradually compacted, the movement of the overlying rock layer also gradually stops, and the sensor indication gradually stabilizes.

4.3 Characteristics of water flow in the overburden

In this test, 10 pore water pressure sensors were set up to monitor the fluid flow characteristics during the mining process. After each excavation, the pore water pressure data are basically stable, and the data from sensors at the different positions are collected to form cloud diagrams of pore water pressure changes in the different mining stages, as shown in Fig. 10. For example, in the fifth step of coal mining, the data monitored by 10 sensors will change. After 20 minutes, the data of the sensor is stable and does not change. We take out the data at the stable time for analysis, and then obtain the Cloud diagrams of the pore water pressure at that time.

In this section, the test results at four key moments, Step 5, Step 7, Step 8, and Step 10, are selected for analysis. It can be clearly seen from Fig. 10 that when Step 5 is excavated, the overburden fracture space has propagated to the pore water pressure sensor area. The first drop in water pressure at P1 indicates that the water pressure is no longer maintained. According to the cloud diagram, the water flows from P1 to P7 (black arrow), which is located above the vertical penetrating crack in the middle of the goaf (above zone (a)). It can be determined that a large amount of surface water or shallow groundwater flows to the working surface (thick red arrow) through the vertical penetrating crack; at the same time, the vertical crack group above the open cut causes part of the groundwater loss (thin red arrow). When the excavation reaches Step 7, the area where the pore water pressure drops gradually expands along with the advancement of the working face, and the groundwater flow range expands. The periodic movement

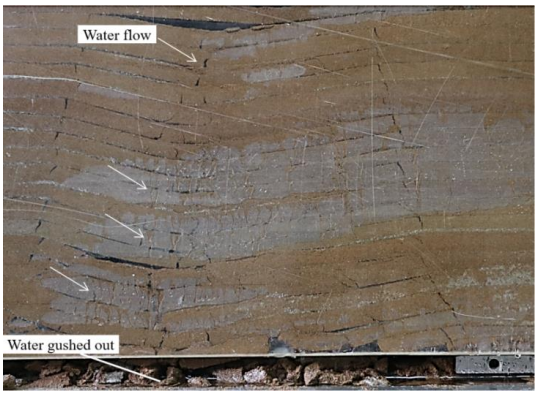

Fig. 11 Flow characteristics of water in the model

of the overburden and the generation of new vertical fracture groups are the main reasons for this phenomenon.

When excavating to Step 8, the sensor data of P6 and P7 decreased, while P3 recovered, which indicates that a stable water inrush channel has been formed in the rectangular area of P1-P2-P5-P6 and caused a large amount of groundwater to break into the goaf (above zone a, water flow is shown in Fig. 11). Affected by the stable water inrush channel, the flow in other areas decreased or disappeared, causing the increase in the pore sensor data. From Step 9 to Step 10, the data of the 10 pore water pressure sensors basically do not change, and the main water inrush channel is still inside the overlying rock above the middle of the goaf formed by the initial weighting.

In summary, with the mining of coal seams, the scope of groundwater flow in the overburden gradually expands. When a stable water inrush channel is formed, new water inrush channels are no longer generated in other areas, and other original channels will be gradually closed. Vertical penetrating cracks formed in the middle of the mined-out area by the initial weighting became the main water bursting channel for the coal mine.

5. Numerical simulation analysis of the overlying rock movement in the inclined direction

To observe the change characteristics of overburden failure degree and nonlinearity in the inclined direction of the working face in detail, this section uses Rocscience Phase2 analysis software and is based on the actual geological conditions of the 52505 working face to establish an inclined mining model (the direction is shown in Fig. 2 A-A`). Phase2 is a finite element software for the elastoplastic analysis of geotechnical engineering problems; it has outstanding advantages in simulating the excavation of underground caverns and can simulate the influence of ore bodies before and after mining occurs on surrounding rock and roadway engineering. Another important function of this software is the use of the Mohr-Coulomb or Hoek-Brown strength criterion for strength-reduced safety factor calculations to determine the breakage of the overburden strata in coal mining.

A working face model was established along the direction parallel to the working face (see Fig. 12), and the spatial parameters of each structure are the same as those of the actual geological data in physical simulation model (see Table 2). The simulated working face in the 5-2 coal seam is 301.3 m long and 6.7 m high, and it was excavated at a depth of approximately 184 m below the ground surface. Note that the modeling was done in 2D and thus is considered to be more conservative than reality because it can lead to a higher stress concentration around the stope. We only use the model to calculate the stress distribution of overburden rock mass after coal mining. The model presents a steady-state solution, and the explicit water flow interactions with the fracture network is not obvious.

The development of the strength factor and failure around the goaf is shown in Fig. 12. The strength factor is the rock strength divided by the rock stress. For a plastic analysis such as this, the strength factor is always greater than or equal to 1 (in an elastic analysis, the strength factor can go below one, as a hypothetical measure of overstress), but the strength factor contours can indicate regions that are close to failure (the lower the value is, the closer to failure). Note that the failure zone corresponds roughly with the zone of the strength factor when it is < 1 from the elastic analysis, with additional propagation beyond this limit, which would be expected from a plastic analysis.

After mining of the 52505 working face, the broken overlying rock occurring in the inclined direction of the working face is symmetrically distributed, as shown in Fig. 12. The immediate roof of the working face has obvious tensile damage, and the surrounding rock of the two crossheadings has shear failure, resulting in the collapse of the immediate roof. The tensile damage area of the main roof within 78.9 m is distributed in a "triangular" shape, and the highest point of the triangular area is located in the middle of the goaf. To observe the discontinuous displacement changes in this area, the vertical displacement characteristics of the overburden over 20~120 m are shown in Fig. 13. The vertical displacement of the rock mass in the "triangular" distribution area affected by plastic deformation shows a sudden increase, indicating that the rock mass is broken. The position above the middle of the goaf of the 52505 working face is therefore determined. The figure shows that the height of the water-conducting fracture zone of the 52505 working face is 78.9 m, which is 11.8 times the mining height.

The indoor rock tests show that when the strength factor is <2, internal cracks are easily generated inside the rock mass, and the width of the cracks is much smaller than the width of cracks in the water-conducting fracture zone. This internal fracture area is shown as a dotted line in Fig. 14 (ubiquitous fracture area). The area is symmetrically distributed, and the lateral span is approximately the length of the working face. At the same time, there is a clear separation between the different rock layers affected by the properties of the rock layer. Notably, the middle part of the ubiquitous fracture area is the narrowest, and the water body above the loose layer will break into the water-conducting fracture zone with the shortest path; thus, the overburden breaking above the middle of the goaf will allow the formation of the water bursting channel.

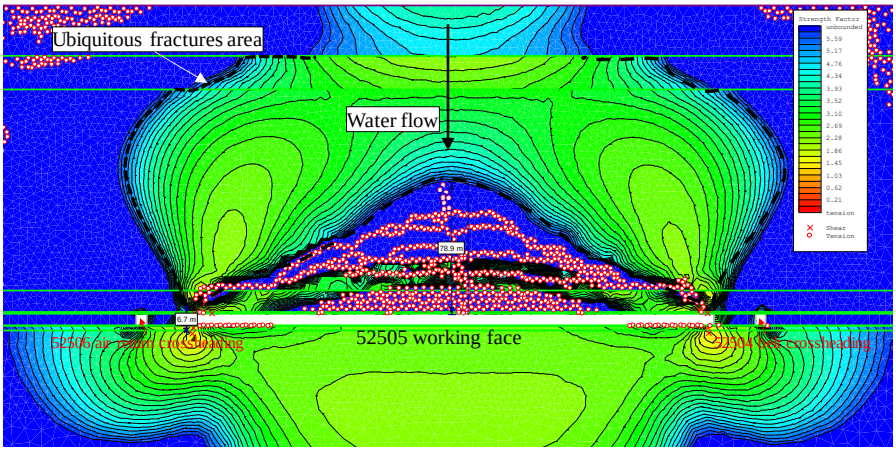

Fig. 13 Strength factor contours and yielded elements. Observe the zone of plastic failure (X shear failure; O tensile failure)

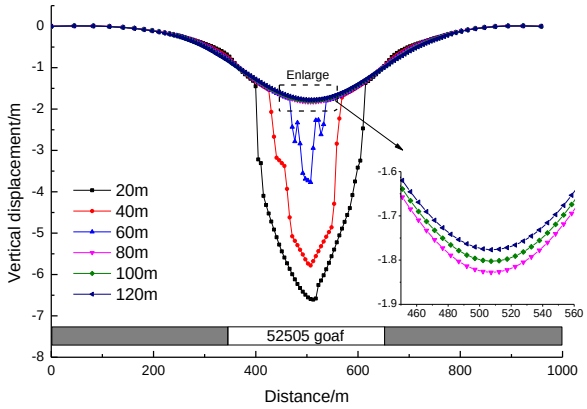

Fig. 14 Variation in the vertical displacement of the overlying rocks at the different distances above the working face

6. Conclusions

- Due to the shallowly buried and weakly cemented soft rock layer in the upper part of the coal seam in West China, the movement of the roof rock layer is particularly sensitive and strong in the horizontal and vertical directions. According to physical tests, the collapse and movement of the overlying strata in shallowly buried and weakly cemented strata have spatiotemporal zoning in the vertical and horizontal directions, and the vertical spatial morphology of the overlying strata is divided into ① the overall migration zone, ② the fracture extension zone, and ③ the collapse zone. The overburden is horizontally divided into the primary fracture zone (a), the periodic fracture zone (b), and the stop-fracture zone (c). Among them, a large range of interlayer fracture groups and vertical penetrating crack groups occur in the primary fracture zone (a), which is the main danger zone for water bursting and sand breaking throughout the mining process.
- From the characteristics of rock mass stress and pore water pressure, the scope of groundwater flow in the overburden gradually expands. When a stable water inrush channel is formed, new water inrush channels are no longer generated in other areas, and other original channels will gradually be closed. Vertical penetrating cracks (zone (a)) formed in the middle of the mined-out area by initial weighting became the main water bursting channels for the coal mine.
- The tensile damage area of the main roof within 78.9 m is distributed in a "triangular" shape, and the maximum vertical displacement is above the middle of the goaf. The fracture area of the overburden is symmetrically distributed, and the lateral span is approximately the length of the working face. The overburden breaking above the middle of the goaf will allow the formation of the water bursting channel, and the water body will break into the water-conducting fracture zone with the shortest path.

In summary, shallow surface water or groundwater break into the goaf through vertical penetrating cracks in the overburden, and the main water inrush channel is located in the overburden above the initial weighting. The key remediation area for grouting reinforcement to prevent the shallow underwater from collapsing is located in the fracture extension zone.

Data availability

The data used to support the findings of this study are available from the corresponding author upon request.

Conflicts of interest

The authors declared that they have no conflicts of interest to this work.

Acknowledgments

This research was financially supported by the Open Fund of State Key Laboratory of Water Resource Protection and Utilization in Coal Mining (SHJT-17-42.14), National

Natural Science Foundation of China (52004147, 51974173), Natural Science Foundation of Shandong Province (ZR2020QE129).

References

Annaidh, A.N., Destrade, M., Gilchrist, M.D. and Murphy, J.G. (2013), "Deficiencies in numerical models of anisotropic nonlinearly elastic materials", *Biomecha. Model. Mechanobiology*, **12**(4), 781-791. https://doi.org/10.1007/s10237-012-0442-3.

Bai, M. and Elsworth, D. (1990), "Some aspects of mining under aquifers in China", *Min. Sci. a Tech*., **10**(1), 81-91. https://doi.org/10.1016/0167-9031(90)90878-V.

Bruce, H. (2020), "Fracturing, caving propagation and influence of mining on groundwater above longwall panels - a review of predictive models", *Int. J. Min. Sci. Technolo.*, **30**(1), 49-54. https://doi.org/10.1016/j.ijmst.2019.12.001.

Chen, S.J., Yin, D., Jiang, N., Wang, F. and Guo, W. (2019), "Simulation study on effects of loading rate on uniaxial compression failure of composite rock-coal layer", *Geomech. Eng.*, **17**(4), 333-342. https://doi.org/10.12989/gae.2019.17.4.333.

Cheng, G., Ma, T., Tang, C., Liu, H. and Wang, S. (2017), "A zoning model for coal mining-induced strata movement based on microseismic monitoring", *Int. J. Rock Mech. Min. Sci*., **94**, 123-138. https://doi.org/10.1016/j.ijrmms.2017.03.001.

Hu, Z., Chen, C., Xiao, W. and Xinjing, W. (2016), "Surface movement and deformation characteristics due to high-intensive coal mining in the windy and sandy region", *Int. J. Coal Sci. Technol.*, **3**(3), 339-348. https://doi.org/10.1007/s40789-016-0144-z.

Khorasani, E., Amini, M., Hossaini, M.F. and Medley, E. (2019), "Evaluating the effects of the inclinations of rock blocks on the stability of bimrock slopes", *Geomech. Eng*., **17**(3), 281-287. https://doi.org/10.12989/gae.2019.17.3.281.

Komurlu, E. and Kesimal, A. (2015), "Sulfide-rich mine tailings usage for short-term support purposes: an experimental study on paste backfill barricades", *Geomech. Eng*., **9**(2), 195-205. https://doi.org/10.12989/gae.2015.9.2.195

Kratzsch, H. (1983), *Mining Subsidence Engineering*. Springer-Verlag, Berlin Heidelberg.

Li, L.P., Chen, D.Y., Li, S.C., Shi, S.S. and Liu, H.L. (2017), "Numerical analysis and fluid-solid coupling model test of filling-type fracture water inrush and mud gush", *Geomech. Eng*., **13**(6), 1011-1025. https://doi.org/10.12989/gae.2017.13.6.1011.

Liao, X., Wei, L. and Hou, J. (2013), "Application of GIS based ecological vulnerability evaluation in environmental impact assessment of master plan of coal mining area", *Procedia Environ. Sci*., **18**, 271-276. https://doi.org/10.1016/j.proenv.2013.04.035.

Lu, W., He, C. and Zhang, X. (2020), "Height of overburden fracture based on key strata theory in longwall face", *PLoS ONE* **15**(1), e0228264. https://doi.org/10.1371/journal.pone.0228264.

Lu, Y., Wang, C., Wang, W., Sun, C. and Zhang, B. (2018), "Height prediction of water flowing fractured zone and thickness effect of long wall caving in thick loose seam with weak cementation in 9th China-Russia symposium", *Coal in the 21st Century: Mining, Intelligent Equipment and Environment Protection*"(COAL 2018) Atlantis Press.

Morrison, K.G., Reynolds, J.K. and Wright, A. (2019), "Subsidence fracturing of stream channel from longwall coal mining causing upwelling saline groundwater and metal-enriched contamination of surface waterway", *Water Air Soil Pollut*., **230**,37(2019). https://doi.org/10.1007/s11270-019-4082-4.

Ning, J., Wang, J., Tan, Y., Zhang, L. and Bu, T. (2017), "In situ investigations into mining-induced overburden failures in close multiple-seam longwall mining: a case study", *Geomech. Eng.*, **12**(4), 657-673. https://doi.org/10.12989/gae.2017.12.4.657.

Elsworth, Z.O. (1993), "Evaluation of groundwater flow into mined panels", *Int. J. Rock Mech. Min. Sci. Geomech.,* **30**(2), 71-79. https://doi.org/10.1016/0148-9062(93)90701-E.

Peng, S.S., Ma, W.M. and Zhong, W.L. (1992), *Surface subsidence engineering*, Society for Mining, New York: SME.

Schubert, J.P. (1980), "Fracture flow of groundwater in coal-bearing strata", *United States: N. p.* 1980. Web.

Song, B., Zhang, S., Zhang, D., Fan, G., Yu, W. and Zhao, Q. (2018), "Inorganic cement grouting for reinforcing triangular zone of highly gassy coal face with large mining height", *Energies*, **11**(10), 2549. https://doi.org/10.3390/en11102549.

Sun, L., Ji H. and Yang B. (2019), "Physical and mechanical characteristic of rocks with weakly cemented strata in Western representative mining area", *J. China Coal Soc.*, **44**(3), 865-873. https://doi.org/10.13225j.cnki.jccs.2018.6039.

Wang, C., Lu, Y., Li, Y., Zhang, B. and Liang, Y. (2019), "Deformation process and prediction of filling gangue: a case study in china", *Geomech. Eng.*, **18**(4), 417-426. https://doi.org/10.12989/gae.2019.18.4.417.

Wang, C., Shen, B., Chen, J., Tong, W. and Li, Y. (2020), "Compression characteristics of filling gangue and simulation of mining with gangue backfilling: an experimental investigation", *Geomech. Eng.*, **20**(6), 485-495. https://doi.org/10.12989/gae.2020.20.6.485.

Whittaker, B.N. and Reddish, D.J. (1989), *Subsidence: Occurrence, Prediction and Control*. Elsevier Science & Technology, Amsterdam.

Zhang, G., Wang, H., Yan, S., Jia, C. and Song, X. (2020), "Simulated experiment of water-sand inrush across overlying strata fissures caused by mining", *Geofluids*, **2020**(8), 1-11. https://doi.org/10.1155/2020/6614213.

Zhang, S.C., Guo, W., Li, Y., Sun, W. and Yin, D. (2017), "Experimental simulation of fault water inrush channel evolution in a coal mine floor", *Mine Water & the Environment* **36**(3), 1-9. https://doi.org/10.1007/s10230-017-0433-9.

Zhang, Y., Tu, S., Bai, Q. and Li, J. (2013), "Overburden fracture evolution laws and water-controlling technologies in mining very thick coal seam under water-rich roof", *Int. J. Min. Science Technol.*, **23**(5), 693-700. https://doi.org/10.1016/j.ijmst.2013.08.013.

CC